



Cite this: *RSC Appl. Interfaces*, 2025, 2, 508

## Formation of all-biopolymer-based composites with cellulose as the main component†

Alexandra S. M. Wittmar, <sup>ab</sup> Oleg Prymak, <sup>c</sup> Thomas Homm, <sup>d</sup> Felix Surholt, <sup>d</sup> Jörg Uhlemann, <sup>d</sup> Natalie Stranghöner <sup>d</sup> and Mathias Ulbricht <sup>ab</sup>

The continuously growing concerns connected to the pollution produced by the extensive use of non-biodegradable composites strongly justify the need to find renewable and bio-degradable alternatives which are able to replace the already established synthetic composite materials. All-biopolymer composites with cellulose as the main component are emerging as excellent replacement candidates, combining full biodegradability with interesting properties. In the present work, such composites containing a cellulose-based textile reinforcement and a biopolymer-based matrix were prepared by two routes: 1) partial dissolution of the reinforcement fibers by impregnation with an ionic liquid (IL) to generate the matrix, or 2) impregnation of the reinforcement with a biopolymer-containing solution in an IL:DMSO mixture as a precursor for the matrix. For both routes, subsequent immersion in water to induce phase separation and thermal drying to complete the lamination yielded the final materials. The influences of the reinforcement textile composition (cotton vs. linen) and matrix generation route as well as the structure of the IL (route 1) or additional biopolymer (cellulose vs. chitosan; route 2) on the composite structure formation and the resulting mechanical properties were investigated in detail. Very high tensile modulus values of  $\sim 2.8 \pm 0.4$  GPa and  $\sim 3.3 \pm 0.4$  GPa were recorded for the composites obtained by the impregnation of a cotton textile with pure ionic liquids 1-ethyl-3-methylimidazolium acetate (EmimOAc) and 1-butyl-3-methylimidazolium acetate (BmimOAc), respectively. The tensile moduli of the composites obtained by the impregnation with BmimOAc were higher than the ones of the composites obtained under the same conditions by the impregnation with EmimOAc. Additionally, the composites obtained by the impregnation of the reinforcement textiles with a diluted solution of a similar biopolymer, namely chitosan, were less hydrophilic, as demonstrated by the increase of the contact angle from below  $40^\circ$  to  $\sim 80^\circ$ .

Received 22nd August 2024,  
Accepted 28th December 2024

DOI: 10.1039/d4lf00300d

rsc.li/RSCApplInter

## Introduction

It was estimated that between 1950 and 2015, more than 6.3 billion tons of plastic waste were generated, among which  $\sim 21\%$  have been recycled or incinerated, and the remaining  $\sim 79\%$  have either been collected in landfills or released into the environment.<sup>1</sup> The highest percentage of plastics, more than 44%, is used for packaging, followed by the use in buildings and constructions ( $\sim 21\%$ ) and consumer and

institutional products ( $\sim 14\%$ ).<sup>2</sup> A strong increase in plastic market share ( $\sim 4.7\%$ ) was observed more recently during the COVID pandemic (2020–2021).<sup>3</sup> It was also estimated that about 32% of the plastic packaging escapes from the collecting system.<sup>1</sup> The wide variety of plastic waste sizes, chemical compositions and properties leads to a great diversity of ways by which they can interact with living organisms: plastics that are considerably larger than the targeted organism can provide substrates for the colonization by microorganisms; larger plastics which are still ingestible have the potential to generate gastrointestinal blockage of the subject which ingested them; smaller ingestible particles which are too small to impose physical risks can still be dangerous by leaching toxic chemicals directly into the organism.<sup>4</sup> For all these reasons, there is continuously increasing interest in studying and trying to find solutions against plastic waste pollution. The number of scientific publications between 2012 and 2021 on this topic increased by a factor of two compared to the number of papers that appeared in the previous decade.<sup>5</sup>

<sup>a</sup> Lehrstuhl für Technische Chemie II, Universität Duisburg-Essen, Universitätsstr. 7, 45141 Essen, Germany. E-mail: alexandra.wittmar@uni-due.de

<sup>b</sup> NETZ – Nano Energie Technik Zentrum, CENIDE – Center for Nanointegration Duisburg-Essen, Carl-Benz-Str. 199, 47057 Duisburg, Germany

<sup>c</sup> Inorganic Chemistry and Center for Nanointegration Duisburg-Essen (CeNIDE), University of Duisburg-Essen, Universitätsstr. 7, 45141 Essen, Germany

<sup>d</sup> Institut für Metall- und Leichtbau, Universität Duisburg-Essen, Universitätsstr. 15, 45141 Essen, Germany

† Electronic supplementary information (ESI) available. See DOI: <https://doi.org/10.1039/d4lf00300d>

To counteract the increasing problems associated with the plastic waste creation, the interest in environmentally friendly and sustainable materials which should replace many glass- or carbon fiber-reinforced polymer-based composites is considerably increasing. Composites with a cellulose matrix and a cellulose reinforcement, the so called “all-cellulose composites” (ACCs), having excellent mechanical properties, are great candidates in replacing conventional synthetic, fossil resource-based composites.<sup>6</sup> Composites where the matrix and reinforcement are constituted from the same or very similar polymers have the great advantage of good compatibility between the two components and, considering their “after life”, the recycling does not require the separation of the components.<sup>7</sup>

For the preparation of ACCs, two main fabrication methods have been distinguished: (1) partial dissolution of a cellulose fabric with the formation of a matrix which laminates the cores of the remaining fibers together, and (2) the complete dissolution of cellulose in an adequate solvent system followed by the impregnation of a cellulose reinforcement material (fibers or fabrics).<sup>8</sup> The first method seems to be more adequate for potential applications because of the improved compatibility between the matrix and reinforcement and the lower shrinkage difference responsible for interfacial void formation.<sup>8</sup> An overview about the manufacturing processes of ACCs from lignocellulose, purified cellulose and cellulose-based textiles was given in 2021 by Haapala *et al.*<sup>9</sup>

One of the most environmentally friendly methods for the fabrication of ACCs is solvent free and involves kraft fibers (2–3 mm) which are dispersed in water after disintegration from sheets and mixed with recycled cellulose pulp, with the mixture being then hot pressed in panels. Optimal levels of fibrillation of the kraft fibers ensure a good balance between the self-binding properties and reinforcing efficiency.<sup>10</sup> More commonly, however, ACCs are produced using solvents adequate for cellulose dissolution, among which the mostly studied ones are *N*-methylmorpholine-*N*-oxide (NMMO), lithium chloride/*N,N*-dimethylacetamide (LiCl/DMAC), NaOH-urea aqueous solution, and ionic liquids (ILs).<sup>11</sup> ACCs have been prepared by partial dissolution of cotton linters in a NaOH/urea mixture, at different temperatures. Sandwiched impregnated cellulose films were immersed in water for cellulose regeneration and finally hot pressed to form the final composite. In that study, the ACCs prepared at  $-10\text{ }^{\circ}\text{C}$  had the best mechanical properties.<sup>12</sup> ACCs have been also prepared by partial dissolution of filter paper with a NaOH/thiourea aqueous solution; the dissolution time, thiourea ratio and processing temperature had a strong influence on the properties of the formed composites.<sup>13</sup> ACCs have been prepared from high-strength rayon by impregnation of the fibers with a cellulose pulp solution in the IL 1-ethyl-3-methylimidazolium acetate (EmimOAc). The generated composites were multi-layered, and the consolidation was realized by heating the stack at 200 mbar at  $80\text{ }^{\circ}\text{C}$  followed by regeneration of cellulose in a water bath and another hot-pressing step. The composites obtained in this way exhibited

mechanical properties comparable to synthetic thermoplastics reinforced with glass fibers.<sup>14</sup> Composite laminates have been also produced by a vacuum infusion technique from used textile fabrics pre-impregnated with a cellulose solution in 1-butyl-3-methylimidazolium acetate (BmimOAc), followed by heating at  $95\text{ }^{\circ}\text{C}$ , coagulation in a water bath and press drying.<sup>15</sup> Huber *et al.* fabricated fiber-reinforced ACC laminates by impregnation with BmimOAc of man-made cellulose textiles or natural linen fibers, followed by hot pressing, coagulation in a water bath and vacuum drying in the hot press. They observed that the dissolution behavior of cellulose fibers was better than that of linen fibers, leading to laminates with better tensile properties due to a more homogeneous fiber–matrix interphase.<sup>16</sup> The superior flexural and impact strength of the ACCs based on rayon textiles resides in the composite structure where all the cellulose fibers are surrounded by a continuous cellulose matrix phase. A crack propagation through the matrix takes place before the fracturing of the fibers occurs. The strong interfacial adhesion between the fibers and the matrix in these materials is the reason for the superior flexural strength.<sup>17</sup> Additionally, the rayon ACCs prepared by solvent infusion processing have proved to have excellent biodegradability, exhibiting a 73% mass loss after 70 days burial under soil.<sup>18</sup> Victoria *et al.* prepared ACCs by partial dissolution of textiles with an EmimOAc:DMSO solvent mixture, hot pressing, coagulation in water and drying by hot pressing.<sup>19</sup> They have shown that by alternating the textile layers with cellulose films, ACCs with improved mechanical properties could be obtained. The EmimOAc:DMSO ratio of the used solvent seems to strongly influence the mechanical properties of the resulting laminates. The highest values of the Young's modulus were obtained for samples prepared with 100% and 80% EmimOAc, while the best peel strength was obtained for the sample prepared with 80% EmimOAc.<sup>19</sup> During the fabrication of single-biopolymer composites *via* solvent infusion into a cellulose textile, the processing parameters dissolution time, dissolution temperature and compaction pressure have been found to play very important roles in the final properties of the laminates. For example, a short dissolution time does not allow a good fiber–matrix adhesion while too long dissolution times result in a too high fraction of the matrix (at the expense of the fiber fraction) and poorer mechanical properties. Higher dissolution temperatures may allow higher fluidization of the liquid, which leads to a better infusion and more dissolution of the cellulose generating materials resulting in improved mechanical properties.<sup>20</sup> By increasing the dissolution time, the void content in the laminate decreases and the adhesion between the laminas improves, leading to enhanced mechanical properties.<sup>13</sup> It was also observed that composites with unidirectionally oriented fibers exhibit mechanical properties superior to the ones of composites with  $90^{\circ}$  oriented fibers. Furthermore, it was demonstrated that the ACCs can be recycled and reused for the preparation of the cellulose matrix in a new textile-based ACC in at least four



cycles.<sup>15</sup> When comparing the mechanical properties of the ACCs with those of similar composites with an epoxy matrix, a slight improvement due to the ionic liquid's action was observed when lyocell fibers were used as a reinforcement. The opposite effect was found when linen fibers were used.<sup>21</sup>

When evaluating the greenness factor of the all-biopolymer-based composites' fabrication with solvents containing ionic liquids and DMSO, several aspects need to be considered. Ionic liquids which are salts with melting points usually below 100 °C, with many of them being liquid also at room temperature, have very interesting characteristics like low freezing points and high boiling points, low flammability and negligible vapor pressure at temperatures up to 400 °C. Such properties made many scientists consider them as green solvents capable of replacing in some processes volatile organic solvents. However, the specialized literature mentions concerns related to the environmental friendliness of the synthesis processes used for the manufacturing of ionic liquids. Additionally, their toxicity and environmental impact are still not completely evaluated.<sup>22</sup> However, positive is the fact that ionic liquids can be recycled and reused.<sup>23</sup> Dimethyl sulfoxide (DMSO) has a relatively high boiling point and low toxicity compared with other organic solvents, but it is known to promote the skin absorption of other toxins and contaminants. On the other hand, cotton- and linen-based textiles are constituted by natural biopolymers, which makes them non-toxic, easily regenerable and bio-degradable. Therefore, the all cellulose-based composites and the all-biopolymer-based composites can also be considered non-toxic and well bio-degradable. For example, certain all-cellulose-based composites exhibited a loss of mass up to 50% by biodegradation after burial in soil for 70 days.<sup>18</sup> Overall, it can be expected that both the all-biopolymer-based composites and their fabrication using an IL/DMSO platform may positively contribute by reducing the ecological footprint of composite materials.

In the present work, we analyse in detail how the two main fabrication routes toward all-cellulose composite laminates can be most advantageously combined with suited process parameters to obtain composites with desired properties. Two types of cellulose-based textiles, one consisting of pure cotton and one consisting of a linen/cotton mixture, were used as reinforcing materials, and the influence of the different solubilities of the two types of fibers in the chosen impregnation liquids on the laminate formation was evaluated. This was aimed at generating a sufficiently high matrix fraction to allow homogeneous void-free binding of the fibers, but without a too advanced dissolution, enabling an efficient use of the mechanical properties of the textile reinforcement. As for certain applications, the water uptake in the laminate should be restricted, and possibilities to reduce the hydrophilicity of the laminate have been evaluated as well. For this purpose, in addition to cellulose, chitosan with medium molecular weight was also investigated as a possible candidate material for the matrix generation when the hydrophobicity of the fabricated composites should be increased.

The present work is relevant because it investigates the structure formation process of all-biopolymer-based composites obtained starting with two different natural biopolymer-based textile reinforcements containing cellulose as the main component. The role played by the presence of additional biopolymers (hemicellulose and lignin) in the composition of the textile with linen during the dissolution and re-precipitation processes in relation to the structure formation and mechanical properties of the generated composites could be revealed. Additionally, this study provides useful information about the general applicability of such fabrication processes when a wider range of biopolymer-based textile reinforcements is aimed to be used for the generation of all-biopolymer-based composites.

## Experimental

### Materials

Two commercially available natural fiber-based textiles, purchased from a local textile store, were used as precursors for the preparation of the all-biopolymer-based composites presented in this study. The first material is a 100% cotton typical household cloth with a specific weight of 102 g m<sup>-2</sup>, while the second material is a linen-containing textile composed of 55% linen and 45% cotton with a specific weight of 153 g m<sup>-2</sup>. The measured thicknesses of the two cloths were ~0.21 mm for the cotton and ~0.34 mm for the linen material. The textiles were cut into pieces with dimensions of 10 (weft) × 10 (warp) cm<sup>2</sup> or 20 (weft) × 10 (warp) cm<sup>2</sup>. The orientation of the fibers in the two materials is presented in the ESI† Fig. S1. Microcrystalline cellulose (Merck Millipore) and chitosan with medium molecular weight, 85% deacetylated (Sigma-Aldrich), were used as received for the preparation of biopolymer-containing solutions. The room temperature ionic liquids 1-ethyl-3-methylimidazolium acetate (EmimOAc) and 1-butyl-3-methylimidazolium acetate (BmimOAc), both in BASF quality (≥95%), were purchased from Sigma-Aldrich. Both ionic liquids are hygroscopic, containing ~1% water. As a co-solvent, dimethyl sulfoxide (DMSO; analytical reagent, assay ≥99.5%) from VWR International was used. As a small fraction of water does not hinder the dissolution of the biopolymers, all solvents were used as received. The precipitation/regeneration of the laminates was performed in regular deionized water, using the non-solvent induced phase separation (NIPS) process, similar to that in some of our previous work.<sup>24,25</sup>

According to the specialized literature, there is a wide range of ionic liquids which are able to dissolve cellulose up to a certain concentration. However, for the intended process it is crucial that the viscosity of the impregnation solvent system is low enough to allow good wetting of and penetration into the textile reinforcement during the processing. Both EmimOAc and BmimOAc are liquid at room temperature and wet well the studied textiles. Additionally, the linen textile contains besides the main component cellulose also hemicellulose and lignin. As demonstrated in other studies, both EmimOAc and BmimOAc are also well suited to dissolve hemicellulose and lignin.<sup>26</sup> A



final argument for the choice of the particular ionic liquids is their availability at a large scale which is mandatory for practical applications. When biopolymer solutions were used for the impregnation of the textile, DMSO addition served to the reduction of the viscosity necessary for good impregnation of the reinforcement material.

### Fabrication procedures

For the fabrication of the composites, the textile cloths were impregnated either with the pure ionic liquids EmimOAc or BmimOAc (route 1) or with an 8% cellulose solution in EmimOAc:DMSO = 30:70 (route 2). A fourth type of impregnation solution consisting of a 1% chitosan solution in EmimOAc:DMSO = 50:50 was additionally used; due to the low biopolymer concentration in the solution, we may consider that also this preparation procedure follows route 1. The dissolved chitosan was mostly used to coat the yarns and to change the hydrophilicity of the final composites and not necessarily to form the matrix. The concentrations of the biopolymers and co-solvent in the impregnation solutions were chosen to generate biopolymer solutions with adequate viscosities.

An 8% cellulose solution in EmimOAc:DMSO = 30:70 was prepared as follows: the amount of cellulose was dispersed first under stirring in DMSO, then EmimOAc was added to the dispersion and stirring was continued until a homogeneous biopolymer solution was obtained.

A 1% chitosan solution in EmimOAc:DMSO = 50:50 was prepared as follows: EmimOAc and DMSO were mixed under stirring. This mixture was inserted in a mortar and ground with the chitosan until a homogeneous paste was obtained. The lump-free paste was transferred in a closed bottle containing a stirring bar and heated under stirring at 70 °C until the complete dissolution of the biopolymer (*ca.* 5 h). An overview on the fabricated all-biopolymer composites is provided in Table 1. For the linen-containing composites, the layers were placed over each other with the same orientation of the linen yarns (*cf.* Fig. S1†).

All samples in this work were obtained by the superposition of three textile layers and were prepared as follows: in the center of a glass plate (10 × 20 cm<sup>2</sup>) a surface area of 10 × 10 cm<sup>2</sup> or 10 × 20 cm<sup>2</sup> was covered with the

desired impregnation liquid by brushing, and then a piece of textile was placed on the wet surface. The textile piece was then allowed to completely suck the impregnation liquid by brushing it with enough viscous fluid. Thereafter, the second layer of textile was added, followed by analogous treatment. After the last textile layer was filled with the impregnation liquid, a second glass plate was added on top and the wet composite was pressed between the two glass plates with the help of fold-back paper clips. The sandwich was then transferred to an oven and heated at 80 °C for 5 h. Thereafter, the wet laminates were left overnight at room temperature to continue the matrix formation. In the next stage, the fold-back clips were removed, and the sandwich was immersed in a water bath at room temperature. After 6 h, the composite could be removed from the glass plates and was then transferred in a fresh water bath at 50 °C where it was left overnight for the completion of the NIPS process.<sup>25</sup>

Thereafter, the samples were washed again several times with fresh water and then pressed again between the two glass plates and ultimately dried in a vacuum oven for 6 h at 60 °C. For the composites with dimensions of 20 × 10 cm<sup>2</sup>, the preparation procedure was analogous.

Fig. 1 presents a schematic description of the processing steps.

### Characterization methods

For the estimation of the density of the textiles and of the laminates, disks with a diameter of 25 mm were cut (three pieces for each material) and weighed. The thickness of the disks was measured in three points with help of a digital micrometer from Mitutoyo Corporation and an average value was further used. The density of the samples was calculated with the following formula:

$$\rho = m/V \quad (1)$$

With *m* – weight in g, and *V* – volume in cm<sup>3</sup> of a disk with a diameter of 25 mm. For each material, the densities of the three disks were determined and average values are presented.

Structural characterization of the composites was realized with help of a light microscope OZL 464 from Kern Optics

**Table 1** Composition of the all-biopolymer composites presented in this work

Material label	Composition	Route
EmimOAc – cotton	Cotton impr. with EmimOAc	1
EmimOAc – linen	Linen impr. with EmimOAc	1
BmimOAc – cotton	Cotton impr. with BmimOAc	1
BmimOAc – linen	Linen impr. with BmimOAc	1
8% Cellulose – cotton	Cotton impr. with 8% cellulose in EmimOAc:DMSO = 30:70	2
8% Cellulose – linen	Linen impr. with 8% cellulose in EmimOAc:DMSO = 30:70	2
1% Chitosan – cotton	Cotton impr. with 1% chitosan in EmimOAc:DMSO = 50:50	1 <sup>a</sup>
1% Chitosan – linen	Linen impr. with 1% chitosan in EmimOAc:DMSO = 50:50	1 <sup>a</sup>

<sup>a</sup> We consider to have here route 1 due to the very low biopolymer concentration in the impregnation solution.



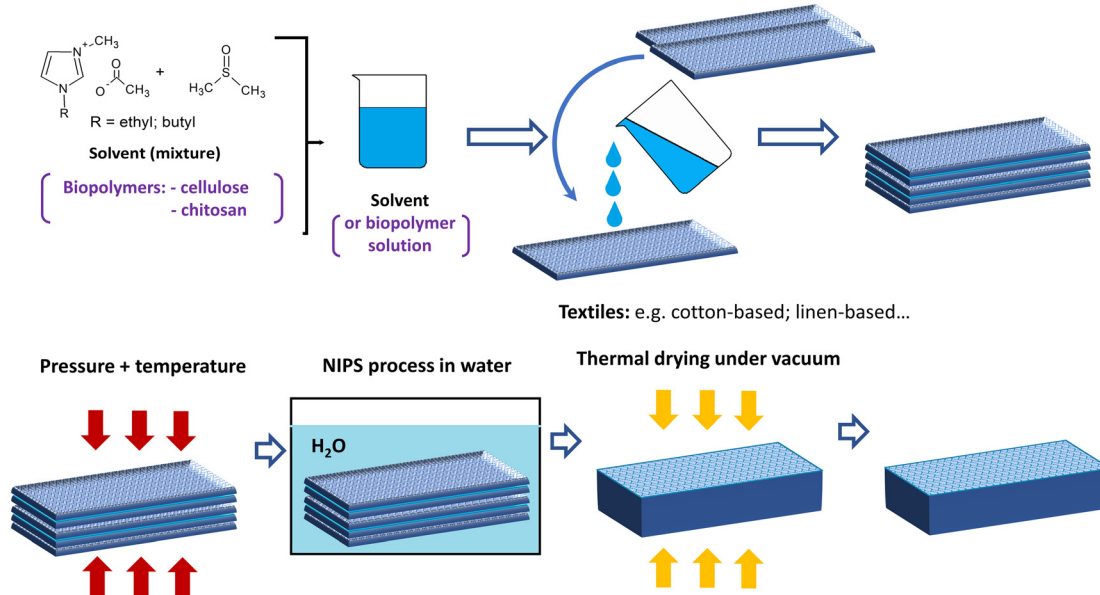


Fig. 1 Schematic description of the main fabrication steps used in the manufacture of the all biopolymer-based composites.

equipped with a Kern ODC 832 camera. The samples were illuminated with a Kern microscope ring light system. The shrinkage during fabrication was estimated by evaluating using the microscope the number of yarns per centimeter, both in warp and weft directions, for the precursor textiles and for the prepared composites. For the cross-section investigation, we used the same disks of 25 mm as for density measurements. The disks were cut with the help of a hole puncher. In order to hold the sample vertically under the microscope, special holders from black plastic were fabricated with a 3D printer. Additionally, the samples were also investigated by scanning electron microscopy using an Apreo S LoVac instrument from Thermo Fisher Scientific. Before the measurement, the samples were sputtered with Au/Pd (80/20) until a 2–3 nm layer was obtained.

Contact angle measurements were performed with an optical contact angle apparatus and using the SCA20 software, both from Data Physics Instruments GmbH, Germany. The contact angle of water in air was measured by the sessile drop method. For each sample, 5 droplets were examined and the resulting mean values and the standard deviations were then calculated.

X-ray diffraction (XRD) was performed with a PANalytical Empyrean instrument in reflection mode using Cu K $\alpha$  radiation ( $\lambda = 1.54 \text{ \AA}$ ; 40 kV, 40 mA). The composite disks were fixed on a flat silicon single crystal sample holder and investigated from 5 to 90° 2 $\theta$  with a step size of 0.007° and a scan speed of 0.024° s $^{-1}$  resulting in a total measurement time of 60 min per sample. The crystallinity index (CI) of the cellulose in the precursor textiles and in the composites was calculated from the XRD spectra using a multi-peak fitting procedure from OriginPro 2022 software which allowed separation of the crystalline and amorphous peaks with Gaussian line shapes. The crystallinity of cellulose was

calculated as the ratio of area corresponding to the crystalline peaks and the total area under the curve in the range 2 $\theta = 10\text{--}30^\circ$ .<sup>27,28</sup> The amorphous contribution was assumed to be a broad peak with the centre at 2 $\theta \sim 21.5^\circ$ .<sup>28</sup>

The mechanical testing of the samples was realized as tensile tests according to ASTM D3039<sup>29</sup> on a Zwick 50 kN Retro Line and on a Zwick 5kN Retro Line testing machine. The conditioning of the specimens was done for 24 h in climate D according to DIN EN ISO 2231:1995-06.<sup>30</sup> The testing parameters were: temperature 23 (±2) °C; test speed 2 mm min $^{-1}$ ; test length 100 mm and measurement of the elongation by recording the traverse travel; preload of 0.5 MPa. For each material, 3 to 5 specimens were tested. Strip specimens with constant width  $b = 10$  mm were used, cut along the general yarn direction yet not completely parallel to the yarns as they were not completely straight due to shrinkage. The stress-strain curves are presented in the ESI† (Fig. S8–S10). For the samples containing linen fibers, the mechanical testing was done along the linen fiber. The evaluation of yield stresses from the test results was accomplished by determining the intersection of tangents applied to the characteristic sections of the stress-strain curves.<sup>31</sup>

## Results and discussion

The analysis of several commercial linen fibers showed that their chemical composition includes cellulose as the main component (~65% up to 82%), hemicellulose (~4% up to ~15%) and lignin (~3.3% up to 8.4%). On the other hand, the cotton fabrics are mainly constituted from cellulose.<sup>32,33</sup> Additionally, it is known that the hydrogen bonds between cellulose, hemicellulose and lignin yield a compact structure which is more difficult to break than the structure created by



hydrogen bonds in the cellulose alone. The ionic liquids chosen for this work are well capable of dissolving both the main component cellulose and the hemicellulose and lignin fraction present in the linen yarn. However, hemicellulose and lignin dissolve better at higher temperatures compared to cellulose.<sup>32</sup> Indeed, preliminary dissolution tests of single cotton and linen yarns in excess ionic liquid at the processing temperature have shown complete dissolution of the cellulose yarn after 1 h and swelling with partial dissolution of the linen yarn after 6 h.

Fig. 2 presents the light microscopy (LM) and scanning electron microscopy (SEM) images of the precursor textile materials used in this work. It can be observed that the cotton cloth is very homogeneous, since the same fibers and yarns have been used in the warp and weft directions. In the case of the linen-containing cloth, the warp yarns are constituted from linen fibers while the weft yarns are constituted from cotton. According to the supplier specification, the linen:cotton ratio in the linen cloth is 55:45. In Fig. 2c, the white yarns are the cotton component, and the brown yarns are the linen component. The fibers constituting the two types of yarns have the same size diameters (Fig. 2d). Experiments with single yarns (not presented here) have shown that the cotton yarns of the “cotton” textile dissolve relatively fast in all impregnation liquids. Slightly slower is the dissolution of the cotton yarns used in the weft direction of the “linen” textiles. The linen yarns are even less soluble and have a tendency to firstly swell. The explanation for their poorer solubility in the ionic liquid-based liquids may be the higher content of non-cellulosic components in linen (~17.3% non-cellulosic content) when compared with cotton (~3.6% non-cellulosic content).<sup>34</sup>

For the precursor textiles, the thickness and density were determined for one layer; for the composite laminates, the respective values were determined for materials constituted from 3 layers of textile. For most of the materials, the thickness of the laminate is lower than the thickness of three

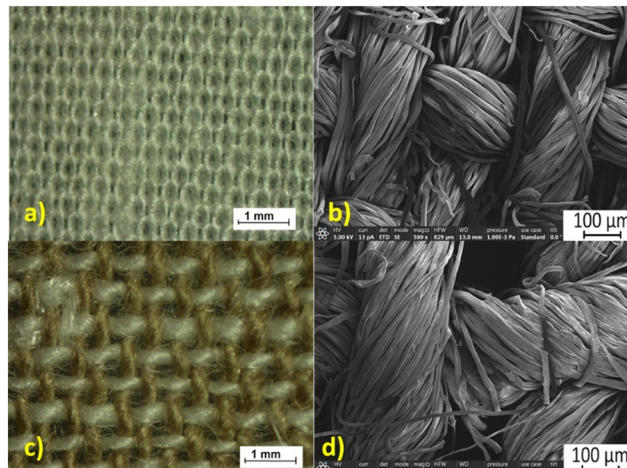


Fig. 2 The surface views by LM (a and c) and SEM (b and d) for the precursor textiles used in this work: (a and b) cotton cloth and (c and d) linen cloth.

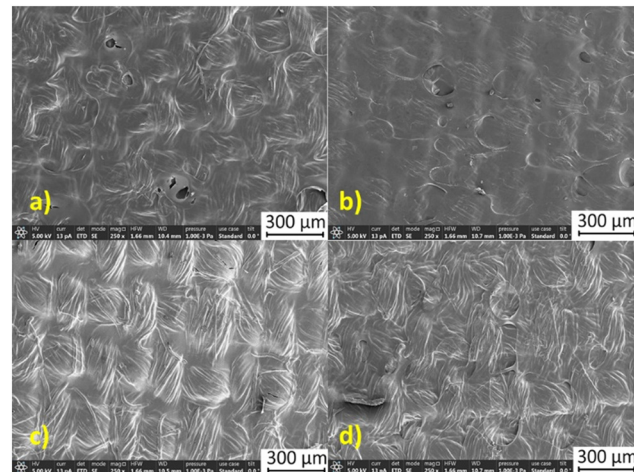


Fig. 3 The surface views (SEM) for the cotton-based composites prepared in this work: a) EmimOAc; b) BmimOAc; c) 8% cellulose and d) 1% chitosan.

superimposed precursor fabrics, suggesting that sintering and rearrangement of the yarns took place during the processing including the final drying step. Fig. 3 and 4 present the scanning electron microscopy images of the composite's surfaces and the densities of the samples are presented in Fig. 5. For both textiles, high density composites were obtained after the impregnation with the pure ionic liquids while the impregnation with 8% cellulose solution led to composites with the lowest density. The densities can be ordered as follows:  $\rho_{\text{BmimOAc}} > \rho_{\text{EmimOAc}} > \rho_{1\% \text{ chitosan}} > \rho_{8\% \text{ cellulose}}$  (Fig. 5).

The light microscopy images of the laminate surfaces are presented in the ESI† (Fig. S2–S5). Impregnation with the pure ionic liquids has led to advanced dissolution of the textile fibers, as suggested by the higher densities of the laminates obtained in this case (Fig. 5a and b). This is also

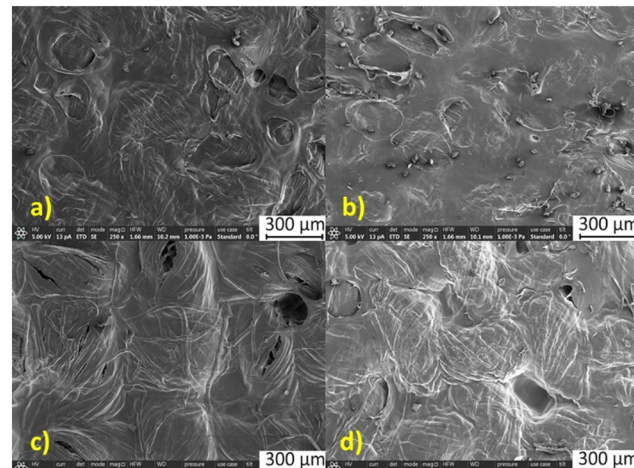


Fig. 4 The surface views (SEM) for the linen-based composites prepared in this work: a) EmimOAc; b) BmimOAc; c) 8% cellulose and d) 1% chitosan.

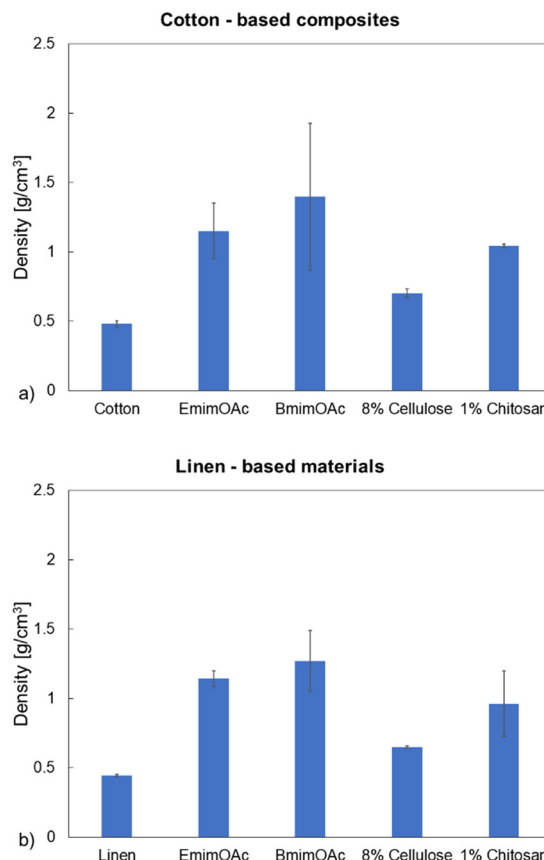


Fig. 5 Density of a) cotton-based and b) linen-containing composites.

clearly observed in the scanning electron microscopy pictures (Fig. 3a and b; 4a and b), where the individual fibers constituting the yarns can only poorly be identified.

The partial dissolution of the fibers in this case leads to the filling of the pores and interstices between the fibers with the dissolved biopolymer, which explains the increase of density. When comparing the action of the two different ionic liquids, both the microscopy images and the values of the estimated densities suggest that BmimOAc dissolves the textile fibers better. The dissolution of the fibers in the 8% cellulose solution in EmimOAc:DMSO = 30:70 was not very advanced due to the relatively low fraction of ionic liquid and due to the saturation of the solution with the biopolymer. However, the interstices between the yarns could be filled with the regenerated cellulose during the phase separation step. Certain regions containing undissolved fibers, covered with reprecipitated cellulose, can be seen in Fig. 3c and 4c.

Nevertheless, the laminates obtained with this impregnation liquid exhibit the lowest density values, which suggests the presence of certain porosity (some cavities) between the undissolved fibers of the yarns covered with reprecipitated cellulose. The poor dissolution of the fibers constituting the yarns for the composites obtained by impregnation with 8% cellulose solution in EmimOAc:DMSO = 30:70 can be also seen in the cross-section of the samples, especially when the “linen” textile was used (Fig. S6c†).

Considering the impregnation with a solution of 1% chitosan in EmimOAc:DMSO = 50:50, a significantly lower concentration of biopolymer in solution and a higher IL fraction compared to the 8% cellulose solution should enable more effective dissolution of the fibers during the process. This is confirmed by a higher density of the produced laminates (Fig. 5) and better dissolution of the fibers. The dense structure and the “sintering” obtained in this case are also recognizable in the cross-section images of the samples (Fig. S3a and S3b; Fig. S5a and S5b†). For some of the samples, it is difficult to identify in the composite the three individual layers due to the partial dissolution of the yarns or due to their rearrangement during the hot-pressing step (Fig. S3 and S5†).

The differences in the densities of the various composites are also a result of the shrinkage during the fabrication process, which here was estimated from the number of yarns per centimetre both in warp and weft directions (Fig. 6). The composites obtained by impregnation with pure ionic liquids exhibit a more pronounced shrinkage than the ones obtained after impregnation with biopolymer solutions. The original shape was better conserved for the composites obtained by impregnation with the 8 wt% cellulose solution in EmimOAc:DMSO = 30:70 compared to 1 wt% chitosan in EmimOAc:DMSO = 50:50. Here the highest impact was imposed by the higher IL fraction. The shrinkage can be ordered as follows:

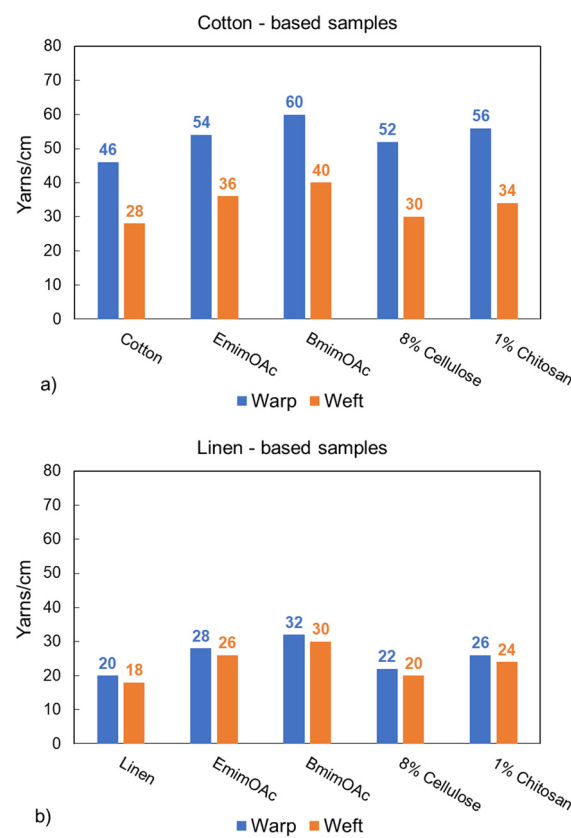


Fig. 6 Number of yarns per centimetre in the dry state for a) cotton-based and b) linen-containing composites.



BmimOAc > EmimOAc > 1% chitosan > 8% cellulose (Fig. 6). All results confirm the dominating effect of a higher efficiency of (partial) fiber dissolution during fabrication on the composite structure formation, leading to more pronounced densification.

The water contact angles of the all-biopolymer composites are presented in Fig. 7. The used precursor textiles are hydrophilic; the contact angles could not be determined because the water droplets were absorbed too fast. All the materials prepared by impregnation with ionic liquids or with cellulose-based solutions maintained their strongly hydrophilic character, exhibiting contact angles below 40°. However, the composites obtained by impregnation with the dilute chitosan solution exhibited a strong increase of the contact angles compared to the precursors. Both functional, hydroxyl- and amino-, groups in chitosan are hydrophilic. Hence, the decrease of hydrophilicity of the composites containing chitosan is most probably caused by a coating of the textile fibers along with a preferential orientation of the hydrophilic groups facing inwards the chitosan film, a structure that can be formed during the gradual drying of the composite.<sup>35</sup> Crystalline cellulose which has the chains packed in the  $I_\alpha$  or  $I_\beta$  crystal structure has an organization of the non-polar structure elements into hydrophobic sheets that are paired against each other, with the regions between the chains controlled by the hydroxyl groups. Such a complex amphiphilic surface is

expected to have a complex hydration behaviour, strongly influenced by the chain hydrophobicity.<sup>36,37</sup> When the composites were fabricated with 1% chitosan solution, the recrystallization of cellulose in the cellulose I crystalline structure seems to have been favoured regardless of the used textile, as also indicated by the XRD spectra (Fig. 8). This may be one of the reasons for the formation of a less hydrophilic surface for those two materials. Here the impregnation solvent was able to dissolve enough cellulose to generate enough matrix so that the surfaces of the formed composites are less influenced by the hydrophilicity of the reinforcement textile.

Fig. 8 presents the diffraction patterns of all precursor textiles and prepared composites. All diffractograms exhibit the characteristic peaks of the cellulose I structure. The diffraction patterns of the composites obtained by impregnation with a cellulose solution are very close to the patterns of the corresponding unmodified textiles. However, most of the composites exhibit also two supplementary features in the diffraction patterns at  $2\theta = 12^\circ$  and at  $2\theta = 20^\circ$  corresponding to the cellulose II polymorph.<sup>38</sup>

In the specialized literature, several methods are used for the estimation of the crystallinity of cellulose in a certain material, amongst which mostly applied are: a) the XRD peak height method, b) the XRD deconvolution method, and c) the XRD amorphous fraction subtraction method.<sup>25</sup> In the present work, the XRD deconvolution method was applied (see the ESI,<sup>†</sup> Fig. S6 and S7) and the calculated crystallinity

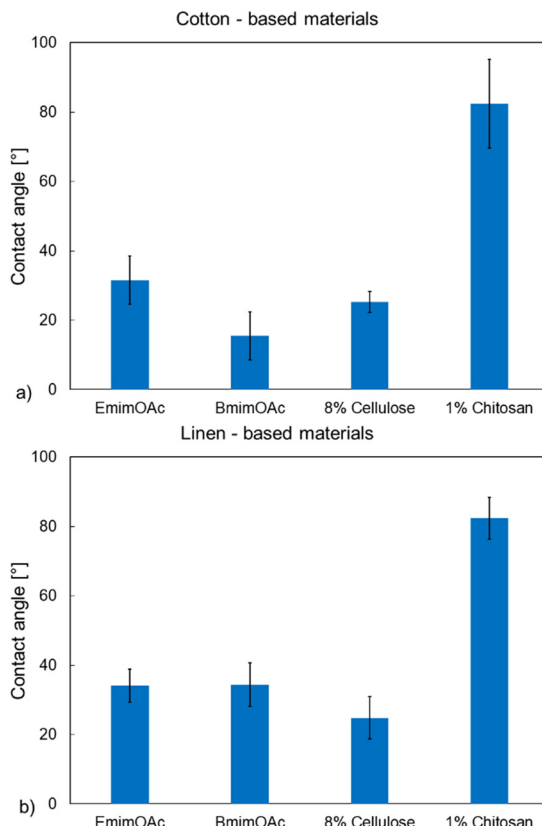


Fig. 7 The water contact angles for a) cotton-based and b) linen-containing composites.

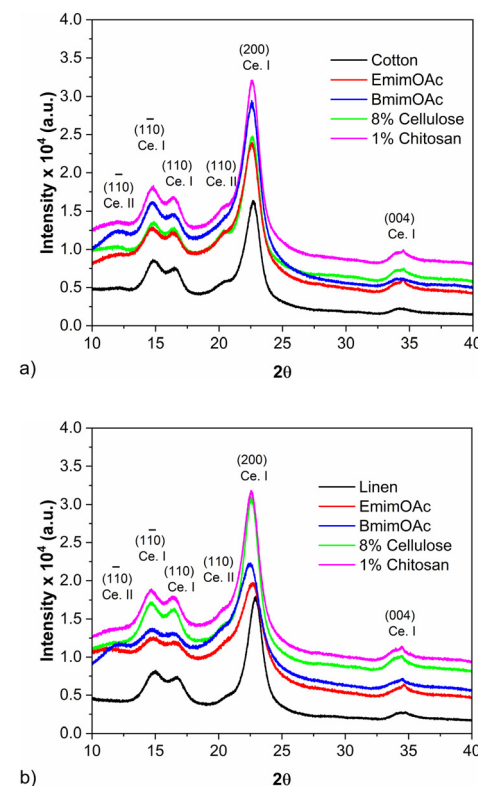
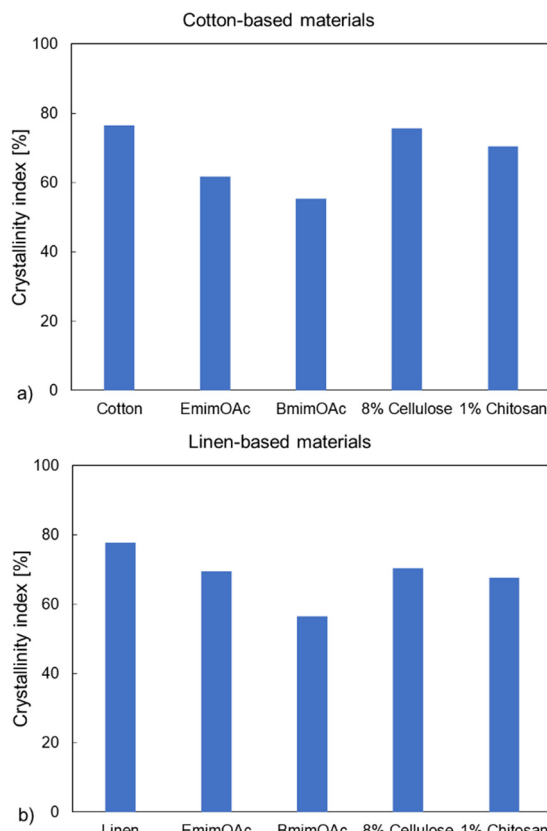


Fig. 8 XRD patterns for precursor textiles and laminar composites: a) cotton-based and b) linen-based.





**Fig. 9** Crystallinity indices (CIs) of precursor textiles and all-biopolymer composites a) cotton-based and b) linen-based, calculated from the XRD patterns.

indices (CIs) of the precursor textiles and of the composites are presented in Fig. 9. As was discussed in the literature, the thus estimated CI of cellulose strongly depends on the method of measurement; therefore, the obtained results provide only a semi-quantitative evaluation of the crystalline or amorphous content in the sample.<sup>27</sup> However, it can offer relevant insights when comparing thus obtained CI data for a series of materials.

The crystallinity of composites obtained by impregnation with a biopolymer solution is relatively high, comparable with the crystallinity of the precursor textiles, while by impregnation with ionic liquids, composites with lower crystallinity are generated (Fig. 9). This is in good agreement with the fact that pure ionic liquids can better dissolve the textiles than the biopolymer solutions, partially converting the fibers into an amorphous matrix during the fabrication process. During the dissolution process, the hydrogen bonds within the cellulose matrix are broken and the original crystalline structure is destroyed; the subsequent coagulation process in water is disadvantageous in terms of recrystallization. In most investigated similar cases, a transformation from cellulose I into cellulose II after the re-precipitation was also observed.<sup>39,40</sup> By analysis of crystallinity, it was also possible to confirm that under otherwise identical process conditions, BmimOAc is able to dissolve the textiles to a higher degree than EmimOAc (Fig. 9).

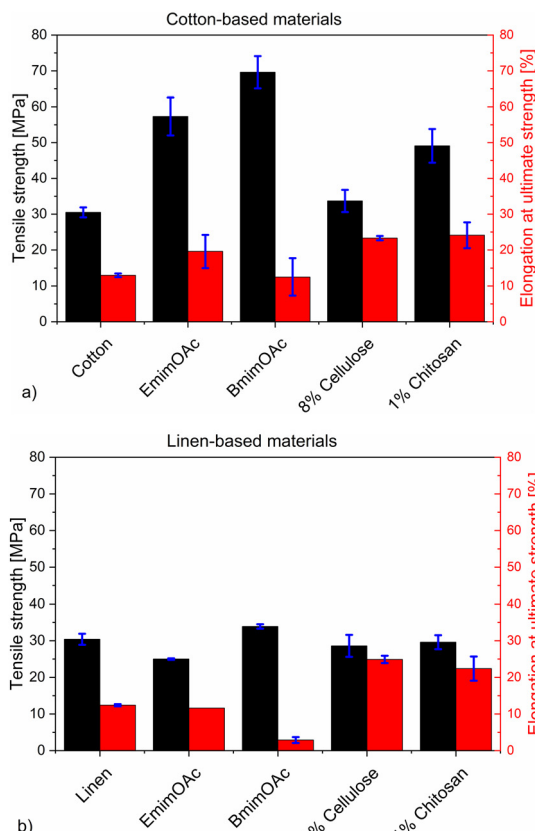


**Fig. 10** Mechanical properties of precursor textiles and all-biopolymer composites a) cotton-based and b) linen-based (precursor materials were measured as a single layer).

The mechanical properties of the precursor textiles and of the prepared composite laminates are presented in Fig. 10. The stress-strain curves are presented in the ESI† (Fig. S8–S10). Although the tensile strength of the linen-containing precursor textile is similar to the data for the cotton-based textile, the tensile strength values of the cotton-based laminates are much higher than those of the corresponding linen-containing laminates. Again, this can be related to the higher non-cellulose content of linen compared to cotton,<sup>34</sup> which has already been discussed above. The cotton-based composite obtained after impregnation with 8% cellulose solution exhibited, however, a value of tensile strength only slightly higher than that of the corresponding linen-based composite, due to the equally poor interaction of the impregnation solution with both of the reinforcing textiles. In the case of the cotton-based composite laminates, superior mechanical properties have been obtained by the first processing route (impregnation with pure ionic liquids). By contrast, in the case of the linen-containing composites, processing with pure ionic liquids has not resulted in an improvement of the tensile strength of the laminates, but it had a considerable effect on the rigidity of the laminate synthesized with BmimOAc: a laminate with low deformation up to fracture was obtained (Fig. 10b). Otherwise, the elongation at ultimate tensile strength is always greater than



that in the precursor textile materials. When comparing the two pure ionic liquids, the laminates generated with BmimOAc have higher tensile strength than the laminates fabricated with EmimOAc (Fig. 10).

A qualitatively different stress-strain behaviour is observed for the composites compared to the precursor materials. While the precursor materials show a very low stiffness in the beginning of the tensile tests up to approximately 6% strain and moderately increasing values afterwards, the composite laminates respond linearly with high stiffness already at low strain. The high initial stiffness probably comes mainly from the matrix, even if the increased yarn density due to shrinkage probably also contributes. All composites except linen-based fabricated with BmimOAc show a pronounced yield point. After roughly 0.5% to 2% elastic strain, a pronounced inflection point in the respective stress-strain curves is observed after which plastic strain occurs up to the elongation at ultimate strength shown in Fig. 10.

Only the linen-based laminate fabricated with BmimOAc breaks before the yield plateau is reached. Table 2 lists the yield stresses and standard deviations of the composite laminates. Conspicuously high values are reached by cotton-based EmimOAc and BmimOAc, with values significantly above the tensile strength of the precursor textile. At the other end, only small values are reached by 8% cellulose, independent of the precursor material. The yield strength of the 1% chitosan materials as well as linen-based EmimOAc is approximately in the middle. Moreover, Table 2 gives tensile moduli for all materials together with the standard deviation observed in the tensile tests. In each case, the tensile modulus is determined as a secant modulus in a defined strain range.

The strain range is defined in such a way that it covers the “service strain” below the yield strain, assuming that – as usual in technical applications – the materials are only utilized in the linear-elastic range up to the yield point. The stress-strain behaviour of the precursor textile materials is not characterized by a yield point, here the service strain is the one up to fracture. The linen-based laminate fabricated with BmimOAc is handled in the same way. However, the precursor materials have a very low stiffness compared to the

composite laminates made of them. When compared with the pure textiles, the stiffness of the 8% cellulose composite laminates is only slightly higher, whereas the linen-based material leads to ~1.5 as much stiffness as the corresponding cotton-based one. 1% chitosan leads to a multiple of stiffness compared to 8% cellulose. The highest stiffness is reached by cotton-based materials processed with pure ionic liquids. In comparison, the stiffness of the linen-based ones processed with pure ionic liquids reaches only roughly half of that.

Overall, there is a clear connection between the solubility of the reinforcement textile in the impregnation liquid and the final properties of the prepared laminates. The higher solubility of the fibers in the pure ionic liquids, especially of the cotton fibers, is clearly indicated by a more pronounced decrease in the crystallinity of the laminates obtained by impregnation with pure ionic liquids (Fig. 9). Due to a slightly lower viscosity of the pure ionic liquids, during their use also a better penetration of the impregnation solution into the textile material is expected, which in turn allows the formation of a larger interface between the matrix and the reinforcement. This is proved by the formation of laminates with higher density (Fig. 5). The stronger packing of the cellulose structure post-drying may also contribute to the much higher tensile strength (Fig. 6). Consequently, the highest density, lowest crystallinity and highest tensile strength were observed for the all-cellulose composite obtained from the cotton-based textile treated with BmimOAc. On the other hand, when the linen-based textile is used as a reinforcement, due to the much lower solubility of the linen in the impregnation liquid, it is expected that the 45% cotton in that textile is most likely to participate in the matrix formation and to bond to the matrix as well. This is indicated also by the lack of improvement of the tensile strength and by a decrease of the values of the elongation at the maximal tensile strength.

Table S1† summarises the most relevant properties of several all-cellulose based composites from the present work and from the specialized literature (please see the ESI† Table S1). Even if the tensile strength value for the best composite obtained in this work (cotton impregnated with BmimOAc) is

**Table 2** Yield stresses and tensile moduli in given strain ranges of the precursor textile materials and the fabricated composite laminates

Material		Yield stress [MPa]	Tensile modulus [MPa]	For strain range [%]
Cotton-based materials	Cotton <sup>a</sup>	—	210 ± 5	0.05–12.0
	EmimOAc	44.0 ± 2.6	2850 ± 404	0.05–1.4
	BmimOAc	54.8 ± 3.7	3338 ± 417	0.05–1.4
	8% Cellulose	3.8 ± 0.7	410 ± 94	0.05–0.7
	1% Chitosan	21.9 ± 3.5	2400 ± 982	0.05–0.7
Linen-based materials	Linen <sup>a</sup>	—	195 ± 12	0.05–11.0
	EmimOAc	24.4 ± 0.6	1502 ± 67	0.05–1.6
	BmimOAc	—	1559 ± 235	0.05–1.7
	8% Cellulose	4.8 ± 0.6	681 ± 88	0.05–0.5
	1% Chitosan	16.3 ± 1.7	2331 ± 86	0.05–0.5

<sup>a</sup> Commercial material.



significantly lower than the tensile strength of the composites reinforced with filter paper,<sup>41,42</sup> it is comparable with the values of other similar composites obtained from rayon fiber textiles or lyocell nonwoven fabric.<sup>16,20,21,43</sup> However, most of these composites require relevantly higher processing temperatures (Table S1†). There is a clear connection between the capacity of an impregnation solution to solubilize the reinforcement textile/nonwoven/paper, at the processing temperature, and the final mechanical properties of the laminates. The hydrogel surrounding the partially dissolved fibers after the re-precipitation with water is pressed in the interstices between the fibers during the drying process leading to “sintering” of fibers. More hydrogel is formed during the processing step, better are filled the interstices between the yarns with reprecipitated biopolymer and a denser composite is formed, leading to materials with high tensile strength. In Table S1,† we can clearly see that all laminates with high values of tensile strength have also relatively high densities. In the case of our samples obtained with a linen reinforcement, the poorer solubility of the linen yarns compared with the cotton ones had as a consequence incomplete filling of the interstices between the yarns with hydrogel and inadequate adhesion of the matrix to the linen yarn. This explains their considerably lower values of tensile strength. These results are in good agreement with similar data obtained when comparing linen/rayon or flax/lyocell textile pairs.<sup>16,21</sup> When a biopolymer solution is used for the impregnation, its interaction with the fiber surface is weaker leading to lower values of tensile strength and lower densities.<sup>44</sup>

When evaluating the crystallinity of the various laminates, we must keep in mind that it is strongly influenced by the cellulose regeneration process with water. The counter-diffusion between the solvent and water during the regeneration process has a strong impact on the re-formation of the hydrogen bonds in cellulose during precipitation. Besides the properties of the used solvents, also the number of layers in such laminates has a strong influence: for thin laminates with only a few layers, the surface to volume ratio is high and the solvent/water exchange is fast. Thicker laminates have slower regeneration leading to higher crystallinities towards the centre.<sup>45</sup> On the other hand, a longer processing time seems to lead to a higher amorphous content.<sup>46</sup>

## Conclusions

We were able to demonstrate that the chemical composition of the cellulose-based textile precursor as well as the composition of the impregnation solvent and the processing method have a very strong influence on the structural and mechanical properties of the prepared all-cellulose-based composites. The tensile strength of the laminates obtained from cotton textiles are much higher than those of equivalent laminates obtained from linen-containing textiles, regardless of the processing method chosen, *e.g.*, ~70 MPa compared

with ~35 MPa when pure BmimOAc was used as the impregnating liquid. This applies similarly to the yield strength, whereby particularly high yield stresses are reached for cotton-based laminates synthesized with pure ionic liquids, *i.e.*, ~44 MPa for the laminate processed with EmimOAc and ~55 MPa for the laminate processed with BmimOAc. Although the processing with pure ionic liquids leads to the formation of laminates with superior tensile and yield strength, this is also accompanied by a stronger shrinkage during the processing up to ~30% for cotton processing with BmimOAc. The composite laminates are generally all considerably stiffer than the precursor textiles, with the 8% cellulose materials clearly standing out at the bottom. Additionally, by processing the laminates with solutions of similar biopolymers, the hydrophilicity of the resulting composites can be changed. For example, composite processing with 1% chitosan has led to an increase of the water contact angles of the composites up to 80°. Overall, we were able to underline and explain how crucial it is to generate during the fabrication of the all-cellulose based composites an adequate amount of compatible matrix (preferably from the same material) in order to generate materials with superior mechanical properties. Additionally, by functionalization of the matrix and/or yarns during the processing with another biopolymer, also other properties of the composite, like hydrophilicity, can be altered.

## Data availability

The data supporting this article have been included in the ESI.†

## Author contributions

Alexandra S. M. Wittmar: supervision, conceptualization, investigation, formal analysis, validation, writing – original draft and introduction. Oleg Prymak: investigation, formal analysis, validation. Felix Surholt: investigation, formal analysis, validation. Thomas Homm: investigation, formal analysis, validation. Jörg Uhlemann: supervision, conceptualization, formal analysis, writing – original draft & editing. Natalie Stranghöner: supervision, writing – review & editing. Mathias Ulbricht: supervision, writing – review & editing.

## Conflicts of interest

There are no conflicts to declare.

## Acknowledgements

We gratefully acknowledge collaboration with Mr. Tobias Bochmann (SEM characterization) at the University of Duisburg-Essen.



## References

1 C. J. Rhodes, Plastic Pollution and Potential Solutions, *Sci. Program.*, 2018, **101**, 207–260, DOI: [10.3184/003685018X15294876706211](https://doi.org/10.3184/003685018X15294876706211).

2 K. L. Low and R. Narayan, Reducing environmental plastic pollution by designing polymer materials for managed end-of-life, *Nat. Rev. Mater.*, 2022, **7**, 104–116, DOI: [10.1038/s41578-021-00382-0](https://doi.org/10.1038/s41578-021-00382-0).

3 G. Kwon, D. W. Cho, J. Park, A. Bhatnagar and H. Song, A review of plastic pollution and their treatment technology: A circular economy platform by thermochemical pathway, *Chem. Eng. J.*, 2023, **464**, 142771, DOI: [10.1016/j.cej.2023.142771](https://doi.org/10.1016/j.cej.2023.142771).

4 F. M. Windsor, I. Durance, A. A. Horton, R. C. Thompson, C. R. Tyler and S. J. Ormerod, A catchment-scale perspective of plastic pollution, *Global Change Biol.*, 2019, **25**, 1207–1221, DOI: [10.1111/geb.14572](https://doi.org/10.1111/geb.14572).

5 A. O. C. Iroegbu, S. S. Ray, V. Mbarane, J. C. Bordado and J. P. Sardinha, Plastic Pollution: A Perspective on Matters Arising: Challenges and Opportunities, *ACS Omega*, 2021, **6**, 19343–19355, DOI: [10.1021/acsomega.1c02760](https://doi.org/10.1021/acsomega.1c02760).

6 *Advanced green composites*, ed. A. Netravali, Scrivener Publishing, Wiley, 2018, pp. 111–133.

7 L. T. T. Vo, B. Siroka, A. P. Manian, H. Duelli, B. MacNaughtan, M. F. Noisternig, U. J. Griesser and T. Bechtold, All-cellulose composites from woven fabrics, *Compos. Sci. Technol.*, 2013, **78**, 30–40, DOI: [10.1016/j.compscitech.2013.01.018](https://doi.org/10.1016/j.compscitech.2013.01.018).

8 B. Baghæi and M. Skrifvars, All-Cellulose Composites: A Review of Recent Studies on Structure, Properties and Applications, *Molec.*, 2020, **25**, 2836, DOI: [10.3390/molecules25122836](https://doi.org/10.3390/molecules25122836).

9 E. K. Uusi-Tarkka, M. Skrifvars and A. Haapala, Fabricating Sustainable All-Cellulose Composites, *Appl. Sci.*, 2021, **11**, 10069, DOI: [10.3390/app112110069](https://doi.org/10.3390/app112110069).

10 N. Soykeabkaew and T. Peijs, Turning low-cost recycled paper into high-value binder-free all-cellulose panel products, *Green Mater.*, 2020, **8**, 51–59, DOI: [10.1680/jgrma.19.00042](https://doi.org/10.1680/jgrma.19.00042).

11 T. Huber, J. Müssig, O. Curnow, S. Pang, S. Bickerton and M. P. Staiger, A critical review of all-cellulose composites, *J. Mater. Sci.*, 2012, **47**, 1171–1186, DOI: [10.1007/s10853-011-5774-3](https://doi.org/10.1007/s10853-011-5774-3).

12 Q. Y. Wei, H. Lin, B. Yang, L. Li, L. Q. Zhang, H. D. Huang, G. J. Zhong, L. Xu and Z. M. Li, Structure and Properties of All-Cellulose Composites Prepared by Controlling the Dissolution Temperature of a NaOH/Urea Solvent, *Ind. Eng. Chem. Res.*, 2020, **59**, 10428–10435, DOI: [10.1021/acs.iecr.9b07075](https://doi.org/10.1021/acs.iecr.9b07075).

13 F. Hu, M. Wang, N. Wang, Y. Hu, M. Gan, D. Liu, Y. Xie and Q. Feng, All-cellulose composites prepared by partially dissolving cellulose using NaOH/thiourea aqueous solution, *J. Appl. Polym. Sci.*, 2021, **138**, e51298, DOI: [10.1002/app.51298](https://doi.org/10.1002/app.51298).

14 J. M. Spörl, F. Batti, M. P. Vocht, R. Raab, A. Müller, F. Hermanutz and M. R. Buchmeiser, Ionic Liquid Approach Toward Manufacture and Full Recycling of All-Cellulose Composites, *Macromol., Mater. Eng.*, 2018, **303**, 1700335, DOI: [10.1002/mame.201700335](https://doi.org/10.1002/mame.201700335).

15 B. Baghæi, S. Compier and M. Skrifvars, Mechanical properties of all-cellulose composites from end-of-life textiles, *J. Polym. Res.*, 2020, **27**, 260, DOI: [10.1007/s10965-020-02214-1](https://doi.org/10.1007/s10965-020-02214-1).

16 T. Huber, S. Pang and M. P. Staiger, All-cellulose composite laminates, *Composites, Part A*, 2012, **43**, 1738–1745, DOI: [10.1016/j.compositesa.2012.04.017](https://doi.org/10.1016/j.compositesa.2012.04.017).

17 T. Huber, S. Bickerton, J. Müssig, S. Pang and M. P. Staiger, Flexural and impact properties of all-cellulose composite laminates, *Compos. Sci. Technol.*, 2013, **88**, 92–98, DOI: [10.1016/j.compscitech.2013.08.040](https://doi.org/10.1016/j.compscitech.2013.08.040).

18 S. Kalka, T. Huber, J. Steinberg, K. Baronian, J. Müssig and M. P. Staiger, Biodegradability of all-cellulose composite laminates, *Composites, Part A*, 2014, **59**, 37–44, DOI: [10.1016/j.compositesa.2013.12.012](https://doi.org/10.1016/j.compositesa.2013.12.012).

19 A. Victoria, M. E. Ries and P. J. Hine, Use of interleaved films to enhance the properties of all-cellulose composites, *Composites, Part A*, 2022, **160**, 107062, DOI: [10.1016/j.compositesa.2022.107062](https://doi.org/10.1016/j.compositesa.2022.107062).

20 M. M. Salleh, K. Magniez, S. Pang, J. W. Dormanns and M. P. Steiger, Parametric optimization of the processing of all-cellulose composite laminae, *Adv. Manuf.: Polym. Compos. Sci.*, 2017, **3**, 73–79, DOI: [10.1080/20550340.2017.1324351](https://doi.org/10.1080/20550340.2017.1324351).

21 W. Gindl-Altmutter, J. Keckes, J. Plackner, F. Liebner, K. Eglund and M. P. Laboie, All-cellulose composites prepared from flax and lyocell fibres compared to epoxy-matrix composites, *Compos. Sci. Technol.*, 2012, **72**, 1304–1309, DOI: [10.1016/j.compscitech.2012.05.011](https://doi.org/10.1016/j.compscitech.2012.05.011).

22 S. S. de Jesus and R. M. Filho, Are ionic liquids eco-friendly?, *Renewable Sustainable Energy Rev.*, 2022, **157**, 112039, DOI: [10.1016/j.rser.2021.112039](https://doi.org/10.1016/j.rser.2021.112039).

23 N. L. Mai, K. Ahn and Y. M. Koo, Methods for recovery of ionic liquids – A review, *Process Biochem.*, 2014, **49**, 872–881, DOI: [10.1016/j.procbio.2014.01.016](https://doi.org/10.1016/j.procbio.2014.01.016).

24 A. S. M. Wittmar, J. Klug and M. Ulbricht, Cellulose/chitosan porous spheres prepared from 1-butyl-3-methylimidazolium acetate/dimethylformamide solutions for Cu<sup>2+</sup> adsorption, *Carbohydr. Polym.*, 2020, **237**, 116135, DOI: [10.1016/j.carbpol.2020.116135](https://doi.org/10.1016/j.carbpol.2020.116135).

25 A. S. M. Wittmar, H. Böhler, A. L. Kayali and M. Ulbricht, One-step preparation of porous cellulose/chitosan macro-spheres from ionic liquid-based solutions, *Cellulose*, 2020, **27**, 5689–5705, DOI: [10.1007/s10570-020-03165-y](https://doi.org/10.1007/s10570-020-03165-y).

26 E. Amini, C. Valls and M. B. Roncero, Ionic liquid-assisted bioconversion of lignocellulosic biomass for the development of value-added products, *J. Cleaner Prod.*, 2021, **326**, 129275, DOI: [10.1016/j.jclepro.2021.129275](https://doi.org/10.1016/j.jclepro.2021.129275).

27 S. Zhang, W. T. Winter and A. J. Stipanovic, Water-activated cellulose-based electrorheological fluids, *Cellulose*, 2005, **12**, 135–144, DOI: [10.1007/s10570-004-0345-2](https://doi.org/10.1007/s10570-004-0345-2).

28 S. Park, J. O. Baker, M. E. Himmel, P. A. Parilla and D. K. Johnson, Cellulose crystallinity index: measurement techniques and their impact on interpreting cellulase



performance, *Biotechnol. Biofuels*, 2010, **3**, 10, DOI: [10.1186/1754-6834-3-10](https://doi.org/10.1186/1754-6834-3-10).

29 ASTM D3039, Standard test method for tensile properties of polymer matrix composite materials, 2014.

30 DIN EN ISO 2231:1995-06, Rubber- or plastics-coated fabrics – Standard atmospheres for conditioning and testing (ISO 2231:1989); German version EN ISO 2231:1995.

31 M. Wu, Y. Li and Y. Shang, Statistical characteristics of ethylene tetrafluoroethylene foil's mechanical properties and its partial safety factors, *J. Mater. Civ. Eng.*, 2016, **28**, 04016004, DOI: [10.1061/\(ASCE\)MT.1943-5533.0001453](https://doi.org/10.1061/(ASCE)MT.1943-5533.0001453).

32 J. Ding, L. Liang, X. Meng, F. Yang, Y. Pu, A. J. Ragauskas, C. G. Yoo and C. Yu, The physiochemical alteration of flax fibers structuring components after different scouring and bleaching treatments, *Ind. Crops Prod.*, 2021, **160**, 113112, DOI: [10.1016/j.indcrop.2020.113112](https://doi.org/10.1016/j.indcrop.2020.113112).

33 M. A. Martins, E. M. Teixeira, A. C. Correa, M. Ferreira and L. H. C. Mattoso, Extraction and characterization of cellulose whiskers from commercial cotton fibers, *J. Mater. Sci.*, 2011, **46**, 7858–7864, DOI: [10.1007/s10853-011-5767-2](https://doi.org/10.1007/s10853-011-5767-2).

34 J. Buchert, J. Pere, L. S. Johansson and J. M. Campbell, Analysis of the Surface Chemistry of Linen and Cotton Fabrics, *Text. Res. J.*, 2001, **71**, 626–629, DOI: [10.1177/004051750107100710](https://doi.org/10.1177/004051750107100710).

35 M. A. Hubbe, Why, After All, Are Chitosan Films Hydrophobic?, *Bioresource*, 2019, **14**, 7630–7631.

36 M. Bergensträhle, J. Wohlert, M. E. Himmel and J. W. Brady, Simulation studies of the insolubility of cellulose, *Carbohydr. Res.*, 2010, **345**, 2060–2066, DOI: [10.1016/j.carres.2010.06.017](https://doi.org/10.1016/j.carres.2010.06.017).

37 H. Miyamoto, U. Schnupf and J. W. Brady, Water structuring over the hydrophobic surface of cellulose, *J. Agric. Food Chem.*, 2014, **62**, 11017–11023, DOI: [10.1021/jf501763r](https://doi.org/10.1021/jf501763r).

38 J. Gong, J. Li, J. Xu, Z. Xiang and L. Mo, Research on cellulose nanocrystals produced from cellulose sources with various polymorphs, *RSC Adv.*, 2017, **7**, 33486, DOI: [10.1039/c7ra06222b](https://doi.org/10.1039/c7ra06222b).

39 S. L. Quan, S. G. Kang and I. J. Chin, Characterization of cellulose fibers electrospun using ionic liquid, *Cellulose*, 2010, **17**, 223–230, DOI: [10.1007/s10570-009-9386-x](https://doi.org/10.1007/s10570-009-9386-x).

40 J. H. Pang, X. Liu, M. Wu, Y. Y. Wu, X. M. Zhang and R. C. Sun, Fabrication and characterization of regenerated cellulose films using different ionic liquids, *J. Spectrosc.*, 2014, **214057**, DOI: [10.1155/2014/214057](https://doi.org/10.1155/2014/214057).

41 T. Nishino and N. Arimoto, All-cellulose composite prepared by selective dissolving of fiber surface, *Biomacromolecules*, 2007, **8**, 2712–2716, DOI: [10.1021/bm0703416](https://doi.org/10.1021/bm0703416).

42 A. Victoria, P. J. Hine, K. Ward and M. E. Ries, design of experiments in the optimization of all-cellulose composites, *Cellulose*, 2023, **30**, 11013–11039, DOI: [10.1007/s10570-023-05535-8](https://doi.org/10.1007/s10570-023-05535-8).

43 B. Adak and S. Mukhopadhyay, A comparative study on lyocell-fabric based all-cellulose composite laminates produced by different processes, *Cellulose*, 2017, **24**, 835–849, DOI: [10.1007/s10570-016-1149-x](https://doi.org/10.1007/s10570-016-1149-x).

44 F. Chen, J. L. Bouvard, D. Sawada, C. Pradille, M. Hummel, H. Sixta and T. Budtova, Explore digital image correlation technique for the analysis of the tensile properties of all-cellulose composites, *Cellulose*, 2021, **28**, 4165–4178, DOI: [10.1007/s10570-021-03807-9](https://doi.org/10.1007/s10570-021-03807-9).

45 J. W. Dormanns, F. Weiler, J. Schuermann, J. Müssig, B. J. C. Duchemin and M. P. Staiger, positive size and scale effects of all-cellulose composite laminates, *Composites, Part A*, 2016, **85**, 65–75, DOI: [10.1016/j.compositesa.2016.03.010](https://doi.org/10.1016/j.compositesa.2016.03.010).

46 B. Adak and S. Mukhopadhyay, Effect of the dissolution time on the structure and properties of lyocell-based all-cellulose composite laminates, *J. Appl. Polym. Sci.*, 2016, **43398**, DOI: [10.1002/APP.43398](https://doi.org/10.1002/APP.43398).

